Noisy zigzag transition, fluctuations, and thermal bifurcation threshold

Jean-Baptiste Delfau, Christophe Coste, and Michel Saint Jean
Laboratoire "Matière et Systèmes Complexes" (MSC), UMR 7057 CNRS, Université Paris 7 Diderot, 75205 Paris Cedex 13, France
(Received 3 April 2013; published 25 June 2013)

We study the zigzag transition in a system of particles with screened electrostatic interaction, submitted to a thermal noise. At finite temperature, this configurational phase transition is an example of noisy supercritical pitchfork bifurcation. The measurements of transverse fluctuations allow a complete description of the *bifurcation region*, which takes place between the deterministic threshold and a *thermal threshold* beyond which thermal fluctuations do not allow the system to flip between the symmetric zigzag configurations. We show that a divergence of the saturation time for the transverse fluctuations allows a precise and unambiguous definition of this thermal threshold. Its evolution with the temperature is shown to be in good agreement with theoretical predictions from noisy bifurcation theory.

DOI: 10.1103/PhysRevE.87.062135 PACS number(s): 05.40.−a, 66.10.cg, 02.30.Oz

Many systems exhibit a topological transition as soon as a parameter β, which controls this transition, reaches a threshold β_{ZZ}. An example of such transitions is the "zigzag bifurcation," which involves a quasi-one-dimensional (1D) chain of interacting particles confined in a narrow channel that forbids any particle crossing [1]. At $T = 0$ K and for an infinite system, the particles remain aligned until the transverse component of the interparticle forces exceeds the transverse confinement, which may be expressed as $\beta > \beta_{ZZ}$ if β is the transverse stiffness [see Fig. 1(a)]. The bifurcation occurs when these two contributions are equal, $\beta = \beta_{ZZ}$. Beyond that, for $\beta < \beta_{ZZ}$, the aligned configuration is energetically unfavorable and mechanically unstable. The linear chain then turns into a 2D zigzag configuration, odd particles up and even down or the symmetric configuration [see Fig. 1(b)].

Experimentally, such transitions and zigzag configurations have been observed in various systems like ions with Coulombic interaction confined in a Paul trap [3,4] or a magnetic Penning trap [5–7], charged particles in a plasma dust interacting with Yukawa interaction [8–11], or colloidal dispersions with screened electrostatic interactions in an annular confinement [12–15]. At the macroscopic scale, we have also observed these zigzag bifurcations with a system of macroscopic metallic beads in electrostatic interaction confined in a finite-sized channel [16] (see Fig. 2).

With negligible thermal noise, the zigzag transition is a supercritical pitchfork bifurcation, which can thus be described in the framework of the Landau theory of second order phase transition. In this formalism, an order parameter which characterizes the topological deformation suddenly changes when a control parameter reaches the bifurcation threshold. Among the possible control parameters, we choose in this Introduction the transverse stiffness β, assuming a fixed density and a fixed longitudinal transverse potential [17]. In this configuration, the transverse distance $|y|$ of the particles to the channel axis increases as the confinement decreases (see Fig. 5). It varies from 0 for $\beta > \beta_{ZZ}$ to a finite value $\langle y\rangle(\beta) = \pm(\beta_{ZZ} - \beta)^{1/2}$ as the difference $\beta_{ZZ} - \beta$ increases. This bifurcation is purely mechanical. The zigzag threshold β_{ZZ} is called the *deterministic threshold* and noted $\beta_{ZZ}(0) \equiv \beta_{ZZ}(T = 0)$.

When the confined particles interact with a thermal bath, the topological properties are no longer sufficient to describe the states of the system. Although the equilibrium configurations are independent of the temperature, the thermal fluctuations directly modify the bifurcation scheme. Far from the threshold, when the system is strongly stable, these fluctuations do not modify the stability of the system, but they have a large influence near the bifurcation since the system is then very sensitive to any small perturbation. In particular, just beyond the deterministic bifurcation threshold [$\beta < \beta_{ZZ}(0)$], the thermal fluctuations allow flips between the two symmetric zigzag orderings; therefore, these two equivalent energetic states are randomly occupied. It results in two important consequences. First of all, these flips induce a temperature-dependent shift of the bifurcation threshold. The Brownian system stays in a single zigzag configuration for $\beta < \beta_{ZZ}(T) < \beta_{ZZ}(0)$ only, where the thermal "lower bound" $\beta_{ZZ}(T)$ characterizes the transverse confinement below which the flips between the energetically equivalent and symmetric zigzag configurations do not happen anymore. The second consequence is a broadening of the variation of $\langle y\rangle$ with β around the threshold $\beta_{ZZ}(0)$, the sharp deterministic bifurcation being replaced by a smooth transition regime for noisy system.

Two interpretations are proposed to analyze these noisy bifurcations. The first one still considers the actual bifurcation as a deterministic transition at $\beta = \beta_{ZZ}(0)$. In this framework the deterministic transition is only blurred by the thermal noise. On the other hand, several studies focusing on the actual particle displacements preferred to introduce a third "bifurcation region" or "mesostate" defined as the range of parameter values $\beta_{ZZ}(T) < \beta < \beta_{ZZ}(0)$ for which the thermal flips control the long time particle dynamics [18–20].

Whatever the description considered, precise determinations of the thresholds are required. The main goal of this article is to discuss the threshold determination in the case of noisy bifurcation. At $T = 0$ K, $\beta_{ZZ}(0)$ corresponds to the value of β for which the singularity is observed in the curve $\langle y(\beta)\rangle$. Let us indicate that for finite systems another method has been proposed: $\beta_{ZZ}(0)$ is characterized by the vanishing of a transverse vibrational frequency of the system [21]. In contrast, for $T > 0$ K, $\beta_{ZZ}(T)$ is not so accurate since the $\langle y(\beta)\rangle$ curve is broadened by the thermal fluctuations which smooth out the

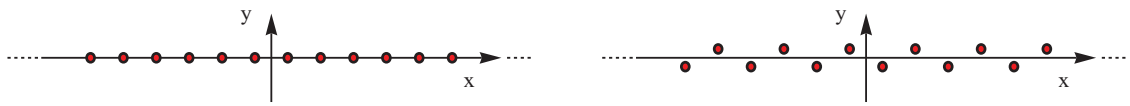

FIG. 1. (Color online) Schematic illustration of the zigzag transition in an infinite system. (Left) Linear configuration; (right) zigzag configuration.

singularity observed at $T = 0$ K. In this case, a lower bound $\beta_{ZZ}(T)$ is usually associated with the inflexion point of $\langle y(\beta)\rangle$ [22]. We propose a new and more accurate determination of $\beta_{ZZ}(T)$ based on the time evolution of the mean square transverse displacements (MSDs) $\langle \Delta y^2\rangle \equiv \langle (y - \langle y\rangle)^2\rangle$ of the confined particles. The transverse MSD saturates at long times. By analyzing the time $\tau_{\rm sat}$ required to reach this saturation value, we show that this time diverges for $\beta \to \beta_{ZZ}(T)$.

This paper is organized as follows. In Sec. I, we describe the behavior of Brownian particles confined in a narrow channel as the transverse confinement varies with the formalism of pitchfork bifurcation. Section II presents the equilibrium configurations obtained by numerical simulations at low temperatures for several values of the control parameters. Their shapes and main characteristics are discussed in the frame of the collective vibrational modes of the system. In particular, we emphasize the contribution of a soft mode near the bifurcation. We focus on systems held in finite boxes, but the Appendix is devoted to the systems with periodic boundary conditions. The specific characteristics of noisy bifurcations are presented in Sec. III. We discuss the failure of the usual procedures to determine the thresholds in Sec. IV. We show how $\beta_{ZZ}(T)$ may be associated with the divergence of the saturation time $\tau_{\rm sat}$ in Sec. V. A conclusion, Sec. VI, summarizes our work.

I. A SYSTEM OF CONFINED INTERACTING PARTICLES

In this paper we focus on the influence of the thermal effects on the bifurcation. In this respect, periodic systems are not very well suited because the thermal fluctuations induce defects in the zigzag structure that can move along the chain [23]. In the following, we are thus interested in finite linear channels with repulsive boundary conditions (RBC) ensured by a longitudinal confining potential. In RBC systems with a long ranged longitudinal confinement [16,24], the particle distribution is very inhomogeneous and the interparticle distances are smaller in the central part of the channel than near its edges [10,16,24]. Thus, the central particles are always the first to reach an interparticle distance $d_{i,i+1}$ smaller than the critical distance $d_{ZZ}(E_{\rm int}, E_w, \lambda_w, \beta)$. When this is the case, a stable "bubble" appears in the central part of the channel while the particles near the cell boundaries remain aligned [9,25]. This stability justifies the choice of RBC systems with a long range confinement for this study. Indeed, for short range confinement, the particle distributions are quasi-homogeneous and look like those of periodic systems. Therefore, the mechanical instability can appear everywhere in the channel and the bubble can move along the particle chain, which results in a less enlightening discussion about the main characteristics of noisy bifurcation.

In order to discuss the noisy pitchfork bifurcation, we have considered interacting punctual and identical particles, submitted to a Brownian noise and confined in a linear narrow channel that forbids any particle crossing.

The repulsive interaction potential between particles is given by

$$V_{\rm int}(\mathbf{r}_i) = E_0 \sum_{j\neq i} K_0\left(\frac{|\mathbf{r}_i - \mathbf{r}_j|}{\lambda_0}\right), \qquad (1)$$

where K_0 is the modified second Bessel function of order 0, E_0 is an energy scale, and λ_0 is a characteristic length [26]. The

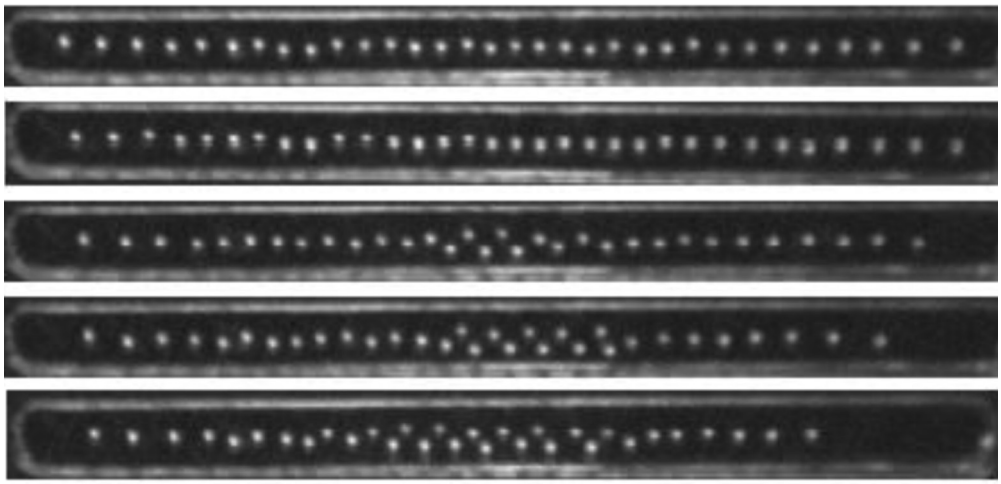

FIG. 2. Example of a zigzag transition in an experimental macroscopic system: 32 metallic beads in electrostatic interaction and confined in a finite-sized channel ($L = 57$ mm) at an effective temperature $T = 9 \times 10^{11}$ K adopt a zigzag configuration as the confinement decreases (from top to bottom).

zigzag transition has also been observed with Yukawa [9,27] as well as with Coulombic potentials [27,28].

Since the particle transverse displacements are small, a symmetric transverse confinement may always be accounted for by a quadratic potential, resulting in a transverse force $F_c^t(y) = -\beta y$. More general y^p confinement potentials have been studied numerically [29,30].

The longitudinal confinement force associated with each side of the finite size channels is given by

$$F_c^l(r) \equiv -\frac{dV_c^l}{dr} = \frac{E_w}{\lambda_w}\left(\frac{\lambda_w \pi}{2r}\right)^{1/2}\left(1+\frac{\lambda_w}{2r}\right)\exp\left(-\frac{r}{\lambda_w}\right), \tag{2}$$

where E_w and λ_w are, respectively, the characteristic energy and the characteristic length of the confinement [31,32]. The interaction with a thermal bath is described in the Langevin formalism, by a dissipative force $-m\gamma\dot{\mathbf{r}}_i$ where γ is the friction coefficient and m the particle mass, and by a random force μ with the properties of a white noise which can be expressed as

$$\langle \mu_x(t)\rangle = 0, \quad \langle \mu_y(t)\rangle = 0, \quad \langle \mu_x(t)\mu_y(t)\rangle = 0, \tag{3}$$

$$\langle \mu_x(t)\mu_x(t')\rangle = \langle \mu_y(t)\mu_y(t')\rangle = 2m\gamma k_B T\delta(t-t'). \tag{4}$$

In these expressions, T is the thermodynamic temperature of the system.

In all simulations, the particle mass is $m = 2.15 \times 10^{-6}$ kg and the dissipation coefficient is $\gamma = 10\ \mathrm{s}^{-1}$. Periodic systems and RBC systems have a length $L = 60$ mm. Unless otherwise stated in the relevant figure captions, the RBC systems are simulated with $N = 33$ particles, $E_w = 0.1E_0$, and $\lambda_w = L/4 = 15$ mm. In specific cases, we vary those parameters in the following ranges: $N \in [31;35]$, $E_w/E_0 \in [0.05;0.15]$, and $\lambda_w \in [0.48;60]$ mm.

The typical length scale that describes the interparticle potential is $\lambda_0 = 0.48$ mm. The typical interparticle energy scale is $E_0K_0[L/(N\lambda_0)] \approx 0.13$ nJ (for $N = 33$), which is conveniently recast as $E_0K_0[L/(N\lambda_0)]/k_B \approx 9 \times 10^{12}$ K. This is to be compared to the thermodynamic temperature T, which varies in the range $T \in [10^2;10^{11}]$ K.

We vary the transverse stiffness in the range $\beta \in [1.07;4.30]$ N/mm. The values of β are mostly chosen to be not too far from the zigzag threshold. They correspond to a typical transverse vibration frequency $\sqrt{\beta/m}$ in the range [22,44] Hz, to be compared to the dissipation $\gamma = 10$ Hz and to the longitudinal cutoff frequency $\sqrt{V_{\mathrm{int}}''[L/(N\lambda_0)]/m} \approx 20$ Hz.

II. EQUILIBRIUM CONFIGURATIONS, BIFURCATION, AND DETERMINISTIC THRESHOLD AT LOW TEMPERATURE

In RBC systems, zigzag bifurcations can be induced either by increasing the transverse interparticle force (by reducing the mean interparticle distance L/N or by increasing the longitudinal confinement energy E_w or characteristic length λ_w) or by decreasing the transverse confinement stiffness β [8,9,30].

At fixed L, β, and (E_w,λ_w), the zigzag bifurcation occurs as soon as the particle number exceeds a value N_{ZZ} [see Fig. 3(a)]. While for smaller N the interparticle distance evolution with the particle rank in the channel is roughly parabolic, for $N > N_{ZZ}$, the distance between the central particles becomes smaller than a critical value d_{ZZ} [see Fig. 4(a)]. At the bifurcation, localized distortions with only one or two particles out of the line have never been observed. The stable configuration is a diamond-shaped bubble involving many particles. As $N > N_{ZZ}$ increases, the central part of bubble grows while its edges remain unchanged in shape. When the density is very

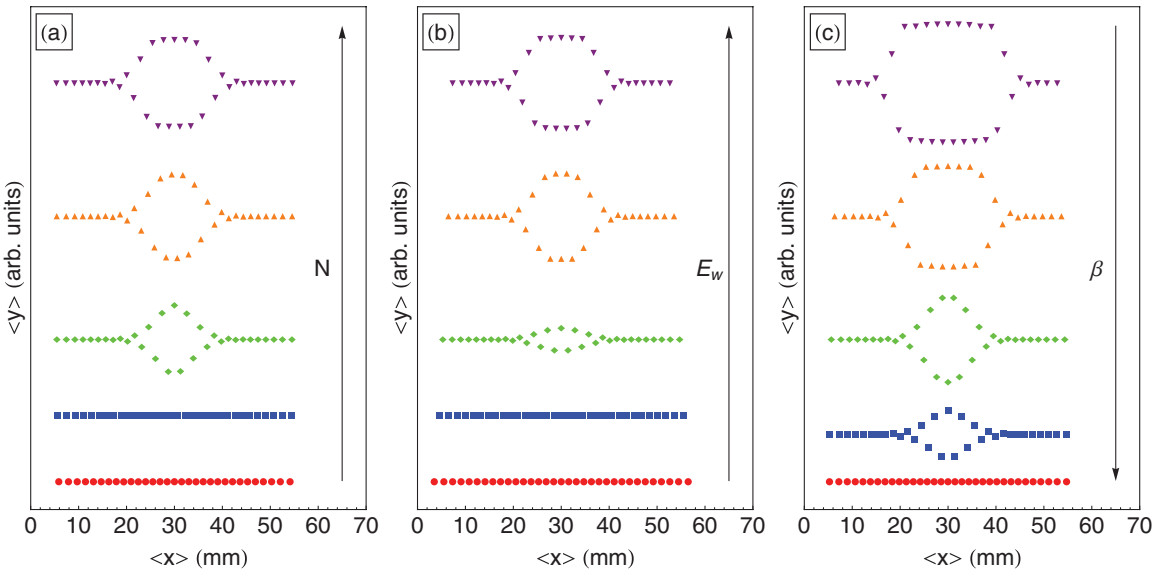

FIG. 3. (Color online) Equilibrium positions of N particles in a RBC system for $T = 10^{11}$ K. (a) Evolution with particle number: $N = 31$ (red circles), 32 (blue squares), 33 (green diamonds), 34 (orange triangles), and 35 (purple triangles); $\beta = 2.04$ N/mm, $E_w = 0.1E_0$. (b) Evolution with longitudinal confinement: $E_w/E_0 = 0.05$ (red circles), 0.075 (blue squares), 0.1 (green diamonds), 0.125 (orange triangles), and 0.15 (purple triangles); $\beta = 2.10$ N/mm, $N = 33$. (c) Evolution with transverse confinement: $\beta = 4.30$ N/mm (red circles), 2.08 N/mm (blue squares), 1.93 N/mm (green diamonds), 1.50 N/mm (orange triangles), and 1.07 N/mm (purple triangles); $N = 33$, $E_w = 0.1E_0$.

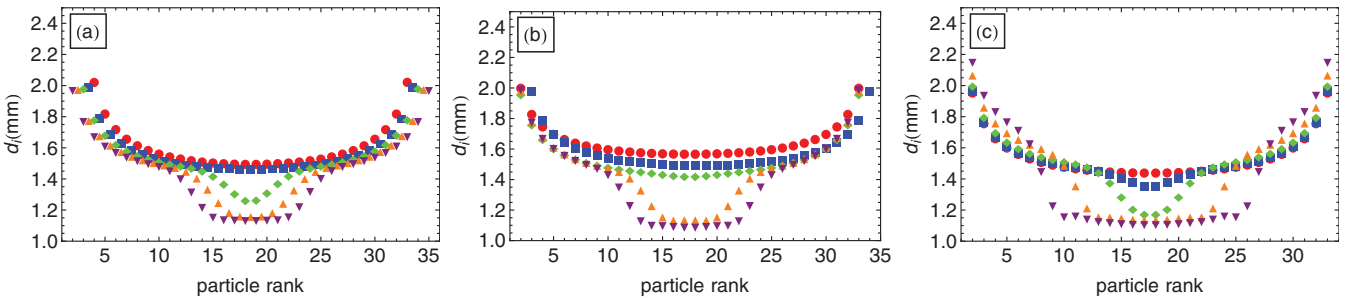

FIG. 4. (Color online) Distance between neighboring particles d_i (mm) as a function of the particle range. We show the dependency of those plots with (a) the particle number, (b) the longitudinal confinement, and (c) the transverse confinement. The color codes and symbol shapes are the same as in Fig. 3.

large, the bubble takes up the whole channel. A secondary bifurcation may then happen, in which the zigzag structure evolves toward a three-line configuration [7]. Qualitatively similar results are observed when the confinement energy E_w or length λ_w exceed critical values E_w^{ZZ} or λ_w^{ZZ} [31] at fixed N, L, and β [see Figs. 4(b) and 3(b)].

The bifurcation can also be controlled by the transverse stiffness β while all other parameters (N, L, E_w, λ_w) are constant, as shown by Fig. 4(c). The system compensates the increase in potential energy due to the transverse confinement by the decrease of interaction energy: In the zigzag bubble, the nearest neighbors are farther apart, and outside the bubble there is also an increase of the interparticle distance, as shown by Fig. 3(c).

In periodic systems, we can write explicitly the normal form [33,34] of the supercritical pitchfork bifurcation that describes the zigzag transition [see Eq. (A2) of the Appendix]. This may be cumbersome with finite RBC systems, but for symmetry reasons the same phenomenology is still valid close to the transition threshold. Let us introduce the dimensionless distance to threshold ϵ, such that $\beta \equiv \beta_{ZZ}(0)(1+\epsilon)$. The mean transverse position of the center particle, which is denoted $\langle y_C \rangle$, is a convenient order parameter, so that the relevant normal form will read

$$m\langle \ddot{y_C} \rangle + m\gamma \langle \dot{y_C} \rangle = \tilde{a}_1 \langle y_C \rangle - \tilde{a}_3 \langle y_C \rangle^3, \quad \text{with} \quad \tilde{a}_1 \propto -\epsilon \quad \text{and} \quad \tilde{a}_3 < 0. \tag{5}$$

Therefore, near the bifurcation the amplitude of the zigzag is such that $\langle y_C \rangle \propto \sqrt{-\epsilon}$. This is observed in Fig. 5, and this allows the determination of the deterministic threshold at low temperature.

Another way to determine the deterministic threshold is associated with the vanishing of the restoring force at the supercritical pitchfork bifurcation [34]. This corresponds to the emergence of a soft mode among the vibrational excitations of the RBC system when the control parameter varies [29,35–40]. The transverse vibrational modes have been calculated in Ref. [21] just above the zigzag transition, when the particles are aligned in their equilibrium configuration [$\beta > \beta_{ZZ}(0)$ or $\epsilon > 0$; in this case the longitudinal and transverse vibrations are uncoupled]. The variations of the eigenfrequencies Ω_s with the mode index s for three values of β are represented in Fig. 6(a). Far from the bifurcation threshold [$\beta \gg \beta_{ZZ}(0)$], the interaction energy is negligible in comparison with the transverse confinement, so that the transverse motions of the particles are roughly decoupled and the corresponding frequency spectrum in Fig. 6(a) is almost flat. As the threshold is approached, the interparticle coupling increases, resulting in the curvature of the frequency spectrum until eventually one frequency vanishes when $\beta = \beta_{ZZ}(0)$ [see Fig. 6(a)]. The vanishing of the lowest frequency Ω_{sm} defines the bifurcation threshold $\beta_{ZZ}(0)$. A plot of $\beta_{ZZ}(0)$ as a function of the characteristic length λ_w of the longitudinal confining potential is shown in Fig. 6(b).

This eigenmodes analysis allows also the prediction of the shape of the zigzag configuration just below the bifurcation threshold. Indeed, the long living soft mode is quenched at the bifurcation, as shown in Fig. 7, where the shape of the soft eigenmode of vanishing frequency is shown to be identical to the zigzag structure just below the transition for $\beta \lesssim \beta_{ZZ}(0)$. This is fully consistent with the description of a supercritical pitchfork bifurcation and means that, strictly speaking, the actual variable that has to be considered in the normal form (5) is not $\langle y_C \rangle$, but rather the amplitude of the soft mode, which is the basis of the center manifold at the bifurcation threshold [33].

Below the transition, $\beta < \beta_{ZZ}(0)$ or $\epsilon < 0$, Eq. (5) describes the dynamics of a particle in a double well of depth

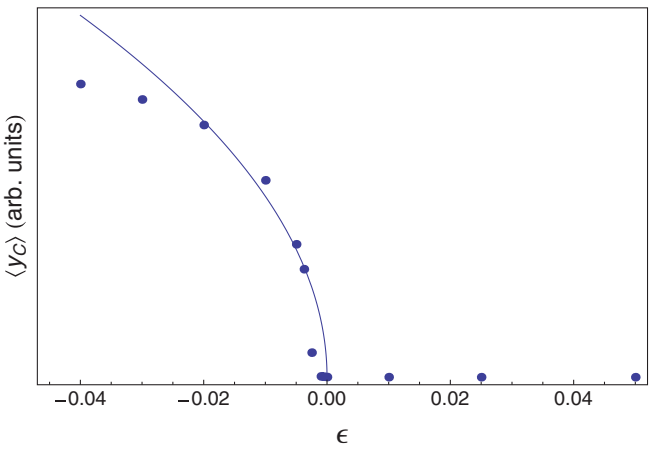

FIG. 5. (Color online) Plot of $\langle y_C \rangle$ (arbitrary units) as a function of the dimensionless distance to threshold ϵ for a RBC system of 33 particles at $T = 10^9$ K confined by a potential with $E_w = 0.1E_0$ and $\lambda_w = 15$ mm. The solid line is a fit $\langle y_C \rangle \propto \sqrt{-\epsilon}$.

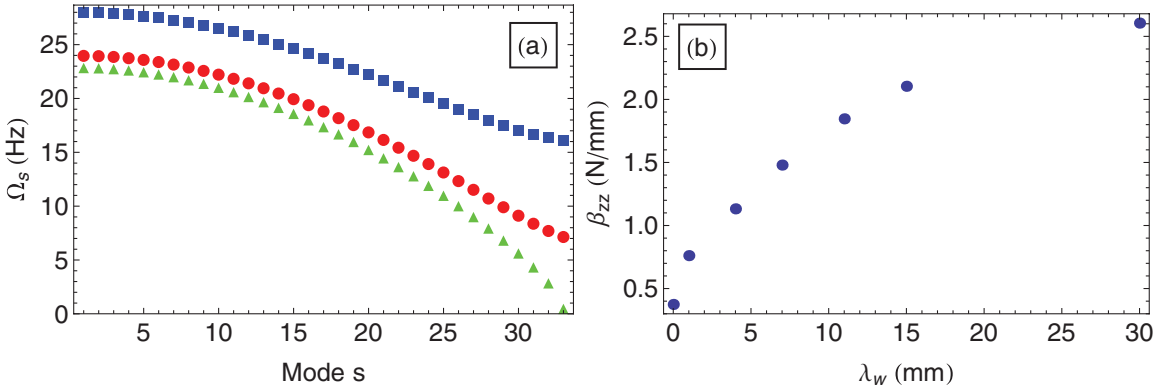

FIG. 6. (Color online) (a) Plot of the eigenfrequencies of transverse vibrations Ω_s (Hz) as a function of the mode index s for a RBC system, with $\lambda_w = 4$ mm and several transverse stiffnesses: $\beta = 1.169$ N/mm (blue squares), $\beta = 1.132$ N/mm (red dots), and $\beta = \beta_{ZZ}(0) = 1.124$ N/mm (green triangles). The soft mode is clearly observable on the green curve: $\Omega_{33} = 0$. (b) Evolution of the deterministic threshold with confinement length λ_w in a RBC system. The value $\lambda_w = 0$ corresponds to a system with periodic boundary conditions.

$\Delta E = \tilde{a}_1^2/(4|\tilde{a}_3|) \propto \epsilon^2$. This phenomenology is recovered for the actual many particle system. In our system, the two equivalent zigzag configurations are the minima of a double well potential with the same energy $E_{ZZ}(\epsilon)$,

$$E_{ZZ} = \sum_{n=1}^{N}\left[V_c^l(\langle x_n\rangle) + V_c^l(L - \langle x_n\rangle) + \frac{\beta}{2}\langle y_n\rangle^2\right] + \sum_{\substack{n,m \\ n\neq m}} V_{\rm int}[\sqrt{(\langle x_n\rangle - \langle x_m\rangle)^2 + (\langle y_n\rangle - \langle y_m\rangle)^2}]. \quad (6)$$

The system, to flip from one configuration to the other, has to cross an energy barrier $\Delta E = (E_{\rm 1D} - E_{ZZ})$, where $E_{\rm 1D}$ is the linear configuration energy,

$$E_{\rm 1D} = \sum_{n=1}^{N}\left[V_c^l(\langle x_n\rangle) + V_c^l(L - \langle x_n\rangle)\right] + \sum_{\substack{n,m \\ n\neq m}} V_{\rm int}\left(|\langle x_n\rangle - \langle x_m\rangle|\right). \quad (7)$$

As expected, ΔE increases when $\beta_{ZZ}(0) - \beta$ increases and varies as ϵ^2 near the deterministic threshold (see Fig. 8).

III. NOISY BIFURCATION AND SHIFT OF THE BIFURCATION THRESHOLD

This bifurcation scheme is deeply modified when the particles are immersed in a thermal bath. The consequences of noise on pitchfork bifurcation is first to blur the deterministic equilibrium positions of the particles and above all to introduce a third new regime between the alignment and the zigzag configuration ones. In order to discuss these effects, it is convenient to consider separately the particle dynamics on both sides of the mechanical bifurcation.

For large enough $\epsilon > 0$, the thermal energy only induces excitations of collective vibrational modes of the chain. The particles oscillate around their equilibrium positions (see the two top plots in Fig. 10) and their transverse fluctuation histograms are thin Gaussian shaped curves, centered on $y = 0$ [see Fig. 9(a)]. Because of the transverse potential well, the transverse MSD at large time saturates to $\sqrt{2k_BT/(m\Omega_{sm}^2)}$, where Ω_{sm} is the smallest transverse oscillations frequency [31,41]. When $\epsilon \to 0^+$, the transverse MSD is dominated by the soft mode contribution; thus, the width of the MSD histogram grows as ϵ decreases [see Fig. 9(b)] and eventually diverges at the bifurcation (see Sec. V and Ref. [21]).

Beyond the bifurcation, $\epsilon < 0$, two different regimes can be identified according to the value of ϵ. For large $|\epsilon|$, such that the two symmetric equilibrium zigzag configurations are

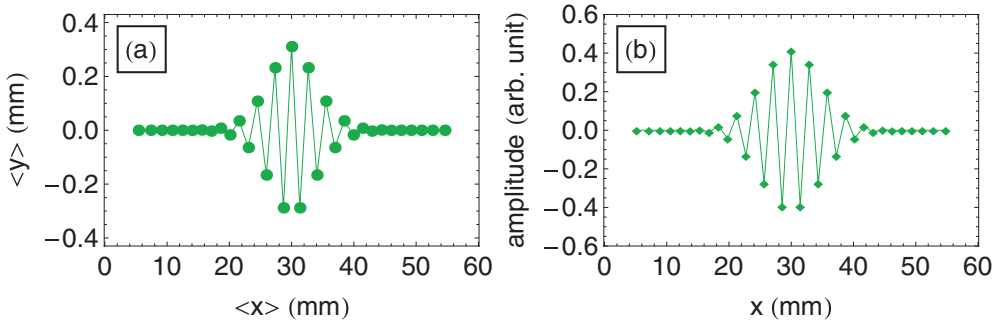

FIG. 7. (Color online) Comparison between (a) the equilibrium configuration observed for $\beta = 2.107$ N/mm at $T = 10^2$ K (no flips are allowed at this low temperature) and (b) the shape of the soft mode amplitude in the RBC system exactly at $\beta = \beta_{ZZ}(0) = 2.602$ N/mm.

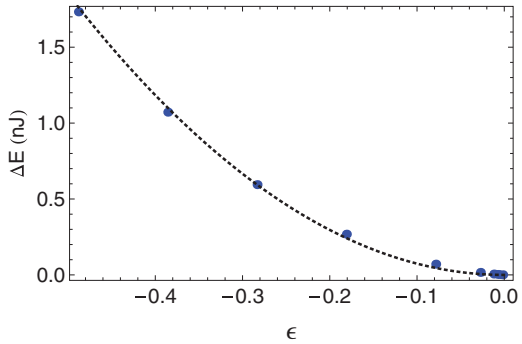

FIG. 8. (Color online) Energetic barrier ΔE (nJ) between the equivalent configurations in the zigzag phase as a function of the dimensionless bifurcation parameter ϵ for the RBC system. This barrier is the energy difference between the linear configuration and the zigzag one observed at $T = 10^2$ K (at this temperature, $\Delta E \gg k_B T$). The dotted line corresponds to a quadratic fit.

separated by an energy barrier that is much higher than $k_B T$, no flips are allowed between those configurations (see the bottom plot in Fig. 10). Each particle stays in the vicinity of only one of its two energetically equivalent equilibrium positions, and the thermal excitations result in vibrations around this position. The histogram of transverse fluctuations then presents only one peak for each particle, centered on its equilibrium position. Notice that its shape is not exactly Gaussian since the local potential explored by the particles is not symmetric [see Fig. 9(f)].

On the contrary, if the system is not far from the deterministic threshold, the energy barrier between the two configurations can be overcome by the thermal energy. The transitions between the two equivalent zigzag configurations are therefore activated and, superposed to the previous vibrational broadening, lead the particle dynamics. However, two different mechanisms have to be distinguished.

Very close to the deterministic threshold $\epsilon \to 0^-$, when the energy barrier between the two equilibrium configurations is such that $\Delta E < k_B T$, these transitions are frequent and continual, as shown in the third plot in Fig. 10, which presents the particle trajectories. The characteristic time associated with each flip (roughly 1 s for the parameters set used in Fig. 10) is of same order than the oscillation time in each equilibrium well. Using the calculations of Meunier *et al.* [18], we may

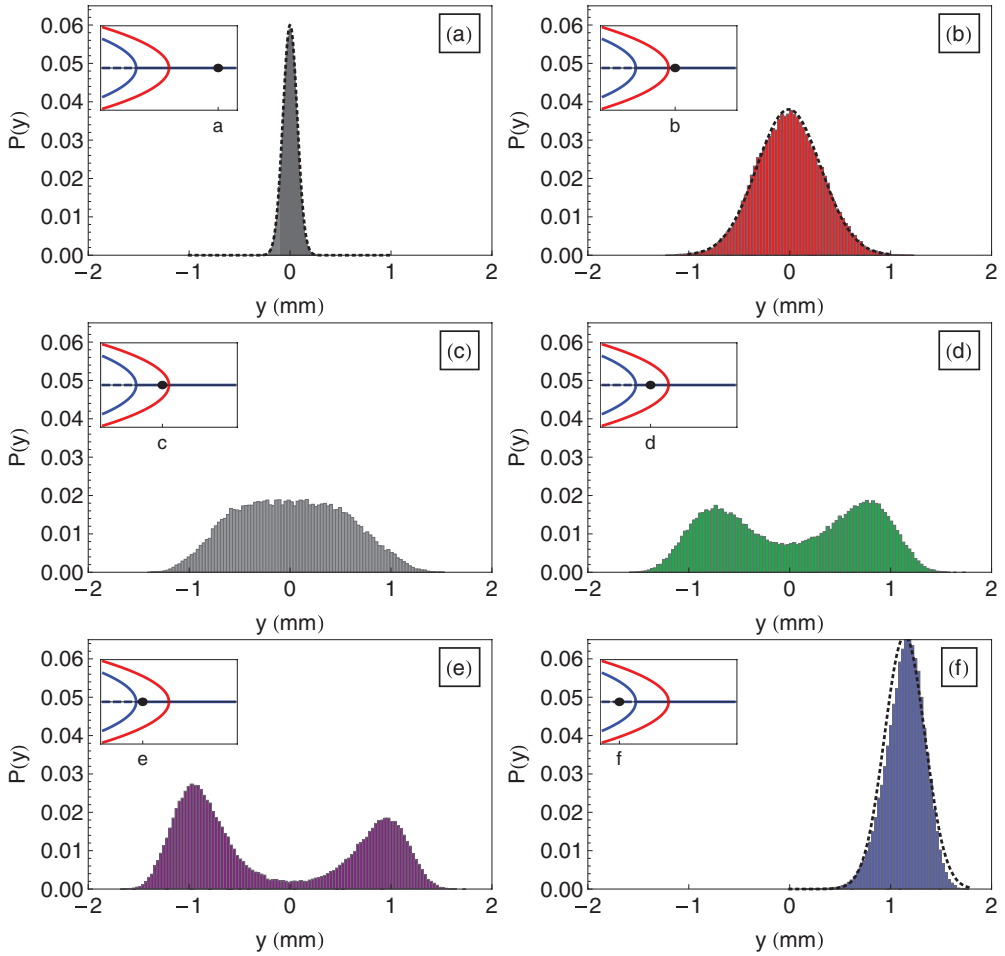

FIG. 9. (Color online) Histograms of the central particle transverse position for the RBC system at $T = 10^{11}$ K. In this configuration $\beta_{ZZ}(0) = 2.10$ N/mm ($\epsilon = 0$, by definition); $\beta_{ZZ}(T) = 2.07$ N/mm ($\epsilon = -0.016$); (a) $\epsilon = 1.05$, (b) $\epsilon = 0.014$, (c) $\epsilon = -0.0003$, (d) $\epsilon = -0.007$, (e) $\epsilon = -0.012$, (f) $\epsilon = -0.027$. In the insets, we plot in red (dark gray) the deterministic bifurcation diagram, whereas the bifurcation diagram that includes thermal effects is plotted in blue (light gray). The large black dot indicates the position of the corresponding ϵ with respect to the thermal and deterministic thresholds. The dotted lines shown in (a), (b), and (f) are Gaussian curves.

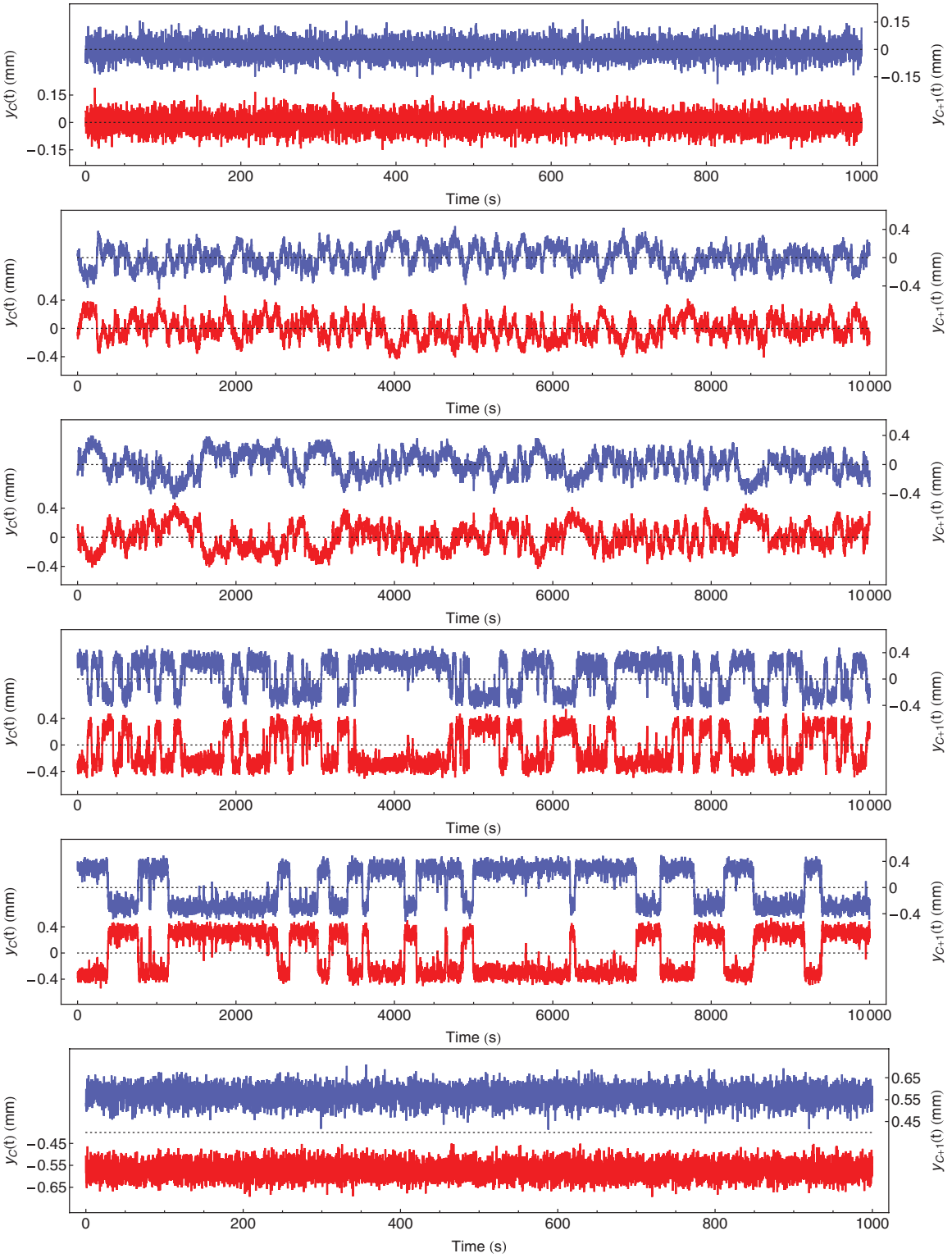

FIG. 10. (Color online) Time evolution of the transverse position of the central particle, $y_C(t)$ (lower red curves, left axis, in mm), and its nearest neighbor, $y_{C+1}(t)$ (upper blue curves, right axis, in mm), in a RBC system at $T = 10^{11}$ K. $\beta_{ZZ}(0) = 2.10$ N/mm; $\beta_{ZZ}(T) = 2.07$ N/mm ($\epsilon = -0.016$). From top to bottom: $\epsilon = 0.13$, 0.001, −0.0003, −0.012, −0.016, and −0.39. The dotted lines correspond to the $y = 0$ axis for each particle. Notice that the particle trajectories are centered on $y = 0$ in the top plot, whereas they are centered on $y \neq 0$ in the bottom plot.

write it as

$$\tau_M \propto \frac{\sqrt{-\epsilon}}{(k_B T)^{3/4}}. \tag{8}$$

In this regime, the histogram of positions is a kind of convolution between the histograms associated with the diffusion around each equilibrium configuration, and the distribution of flips between equivalent configurations. The result is a

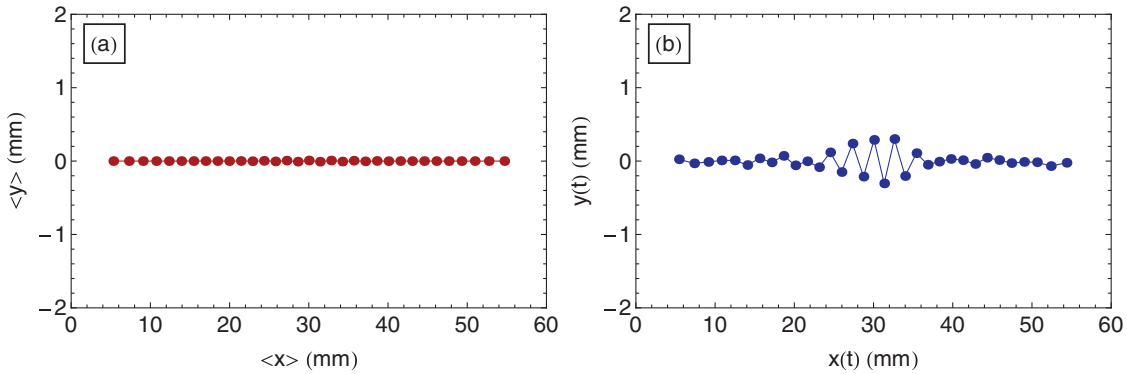

FIG. 11. (Color online) Comparison between the equilibrium and the instantaneous positions of a RBC system with $\epsilon = -0.018$ and $T = 10^{11}$ K. (a) Equilibrium positions $(\langle x\rangle, \langle y\rangle)$ (mm); (b) instantaneous position $(x(t), y(t))$ (mm).

large and not Gaussian curve which remains symmetric with respect to $y = 0$ [see Fig. 9(c)], in agreement with previous studies [18,42].

When the energy barrier between the two equilibrium configurations is such that $k_B T < \Delta E$, the flips between the two energy minima are not so frequent since the thermal fluctuations rarely allow the crossing of the energy barrier, as can be seen from the particle trajectories (see the fourth and fifth plots in Fig. 10). In this limit, the characteristic time of the flip transitions, τ_K, may be estimated from the Kramers formalism [43], as

$$\tau_K = \frac{\sqrt{2}m\pi\gamma}{\beta(0)|\epsilon|} \exp\left(\frac{\Delta E}{k_B T}\right). \tag{9}$$

In this case, the particles can diffuse around each of their available equilibrium positions so that two quite well separated peaks can be observed on the histogram of positions [see Figs. 9(d) and 9(e)].

As shown in Eq. (9), the Kramers time strongly increases with $|\epsilon|$ because in the exponential term ΔE increases as $|\epsilon|^2$. For a lower bound $\epsilon(T) = \beta_{ZZ}(T)/\beta_{ZZ}(0) - 1$, this time becomes higher than the experimental time and the system seems quenched in an single configuration. The histogram of positions then presents a single asymmetric curve describing the diffusion in only one potential well [see Fig. 9(f)].

From the analysis of these histograms, three different regimes clearly appear according to the confinement parameter β. Between the regimes $\beta > \beta_{ZZ}(0)$ and $\beta < \beta_{ZZ}(T)$ for which the system stays in a single equilibrium configuration, a third regime $\beta_{ZZ}(T) \leqslant \beta \leqslant \beta_{ZZ}(0)$ can be exhibited as soon at $T > 0$ K, in which transitions between zigzag equilibrium configurations are relevant. This intermediate regime, named the *bifurcation region* ([18]; we use this denomination henceforward, particularly in Sec. V) or *mesostate* [20], is characteristic of the noisy bifurcation. Qualitatively, the threshold appears to be shifted from $\beta_{ZZ}(0)$ towards $\beta_{ZZ}(T) < \beta_{ZZ}(0)$. It is therefore named the *thermal threshold* hereafter.

IV. ON SOME ATTEMPTS TO DETERMINATE A THRESHOLD FOR NOISY BIFURCATION

At low temperature $[E_{\text{int}}(\bar{d}) \gg k_B T]$, since the bifurcation can be mapped to a second order transition, the deterministic threshold $\beta_{ZZ}(0)$ is associated with a singularity in the $\langle y_C(\beta)\rangle$ curve, as indicated before. However, the threshold determination formally requires an ensemble average of the order parameter. In practice, in experiments or simulations, this ensemble average is replaced with an average calculated over a finite time τ_{av}. Therefore, this ergodic assumption is valid only if the system can explore all of its configurations a large number of times during τ_{av}. This weakens the precise determination of $\beta_{ZZ}(0)$. Indeed, the condition $\tau_{\text{av}} > \tau_r$, where τ_r is the relaxation time $m\gamma/[|\epsilon|\beta_{ZZ}(0)]$, forbids approaching $\beta_{ZZ}(0)$ closer than $m\gamma/\tau_{\text{av}}$. Thus, for systems with small dissipation γ and large average time τ_{av}, $\beta_{ZZ}(0)$ can be determined from the $\langle y_C(\beta)\rangle$ curve. It is not the case otherwise.

A similar procedure is often used at higher temperature $[E_{\text{int}}(\bar{d}) \approx k_B T]$. However, in this case, the $\beta_{ZZ}(0)$ determination is even more tricky. Near the bifurcation, the particle dynamics is led by the soft mode oscillations of period $1/\Omega_{sm}$ that increases as β decreases towards $\beta_{ZZ}(0)$. Therefore, near the bifurcation $[\beta > \beta_{ZZ}(0)]$, $1/\Omega_{sm}$ may become higher than the averaging time τ_{av}, so that the ergodicity assumption is broken and $\langle y_C\rangle$ may differ from its expected null value, suggesting a bifurcation threshold higher than the actual one. So in order to obtain the best determination of $\beta_{ZZ}(0)$, it would be necessary to consider the largest possible average

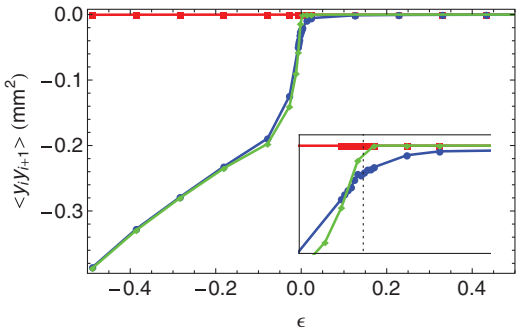

FIG. 12. (Color online) Variation of the pair correlation function $\langle y_i y_{i+1}\rangle$ (mm^2) with the dimensionless transverse confinement ϵ in a RBC system. For the central particle: $T = 10^2$ K (green or very light gray curve); $T = 10^{11}$ K (blue or medium grey curve). For an outermost particle: $T = 10^{11}$ K (red or dark gray curve). The inset focuses around the deterministic threshold $\epsilon = 0$; the dotted vertical line indicates its position.

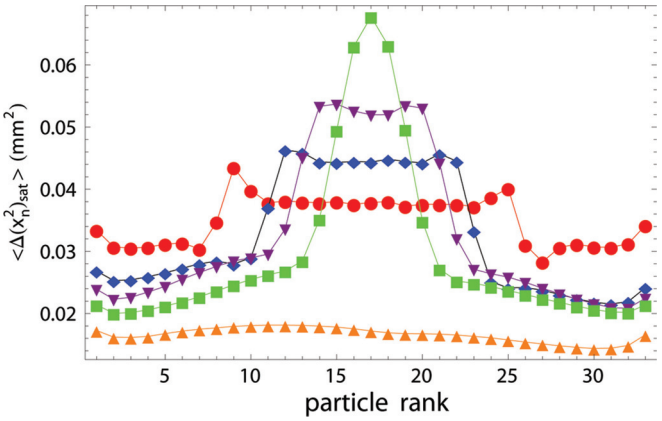

FIG. 13. (Color online) Saturation values of the longitudinal mean square displacement $\langle \Delta x_n^2 \rangle_{\rm sat}$ (mm^2) according to the particle index n in the RBC system at $T = 10^{11}$ K. In this configuration $\beta_{ZZ}(0) = 2.10$ N/mm; $\beta_{ZZ}(T) = 2.07$ N/mm. Transverse confinements are $\beta = 1.075$ N/mm (red dots), $\beta = 1.505$ N/mm (blue diamonds), $\beta = 1.72$ N/mm (purple triangles down), $\beta = 1.935$ N/mm (green squares), and $\beta = 2.15$ N/mm (orange triangles up).

time $\tau_{\rm av}$. However, just beyond the bifurcation, the dynamics is led by the rapid configuration flips characterized by τ_M. So if $\tau_{\rm av} > \tau_M$, $\langle y_C \rangle$ will vanish although $\beta < \beta_{ZZ}(0)$. This is shown by the comparison between the averaged configuration over $\tau_{\rm av}$ obtained for $\epsilon = -0.018$ and an instantaneous one provided by Fig. 11. The averaged configuration looks like an alignment, whereas the instantaneous one exhibits a zigzag bubble. Similar behaviors exist as long as β is in the "bifurcation region." So, to obtain $\langle y_C \rangle \neq 0$ when $\beta \to \beta_{ZZ}(0)^-$, it would be necessary to take small $\tau_{\rm av}$.

Therefore, a precise determination of the deterministic threshold requires two contradictory conditions: $\tau_{\rm av}$ has to be larger than Ω_{sm}^{-1}, which diverges at the bifurcation but smaller than τ_M, which vanishes. In practice, the thermal bath blurs the bifurcation as shown in Fig. 4 and the procedure using the singularity in the $\langle y_C(\beta) \rangle$ curve misses the deterministic threshold [38,44].

To circumvent this difficulty, we could be tempted to consider the correlation function of the displacements of two neighboring particles as the order parameter. We may expect that this observable vanishes when $\beta > \beta_{ZZ}(0)$ and differs from 0 otherwise since the rapid changes of configurations induce simultaneous permutations of neighboring particles. This is indeed the case at low temperatures, but when the temperature increases the correlation does not strictly vanish when $\beta > \beta_{ZZ}(0)$, which shows that the transverse fluctuations are correlated above the deterministic zigzag threshold. This is clearly illustrated on Fig. 12, which shows the variations of $\langle y_C y_{C+1} \rangle$ for the central particle measured at $T = 10^2$ K and $T = 10^{11}$ K. Thus, these two simple procedures to measure the deterministic threshold in noisy bifurcations are unsuitable at finite temperature.

V. DETERMINATION OF THERMAL THRESHOLD AND TRANSVERSE MSD

In this section, we show the consequences of the zigzag transition on the longitudinal and transverse MSD, $\langle \Delta x_n^2(t) \rangle$ and $\langle \Delta y_n^2(t) \rangle$. In particular, we focus on the ability of the transverse MSD behavior to provide the most sensitive and unambiguous way to define the bifurcation threshold when thermal fluctuations are not negligible.

The transient variations of the longitudinal and transverse MSD have been previously discussed in Refs. [21,32]. In finite RBC systems, they both saturate at large times. The saturation values $\langle \Delta x_n^2 \rangle_{\rm sat}$ and $\langle \Delta y_n^2 \rangle_{\rm sat}$ as well as the saturation times $\tau_{\rm sat}$ strongly depend upon the confinement stiffness β, which makes the bifurcation clearly observable on the saturation values.

The variations of $\langle \Delta x_n^2 \rangle_{\rm sat}$ with the particle index n are shown in Fig. 13 for several values of β. For $\beta \gg \beta_{ZZ}(0)$, $\langle \Delta x_n^2 \rangle_{\rm sat}$ is small and roughly independent of n except for the outermost particles for which we can observe a fluctuation enhancement [31]. Just beyond the bifurcation, $\beta \to \beta_{ZZ}(0)^-$, the MSD associated with particles in the zigzag bubble are larger, the largest being associated with the central particle. This is qualitatively explained by the fact that these particles

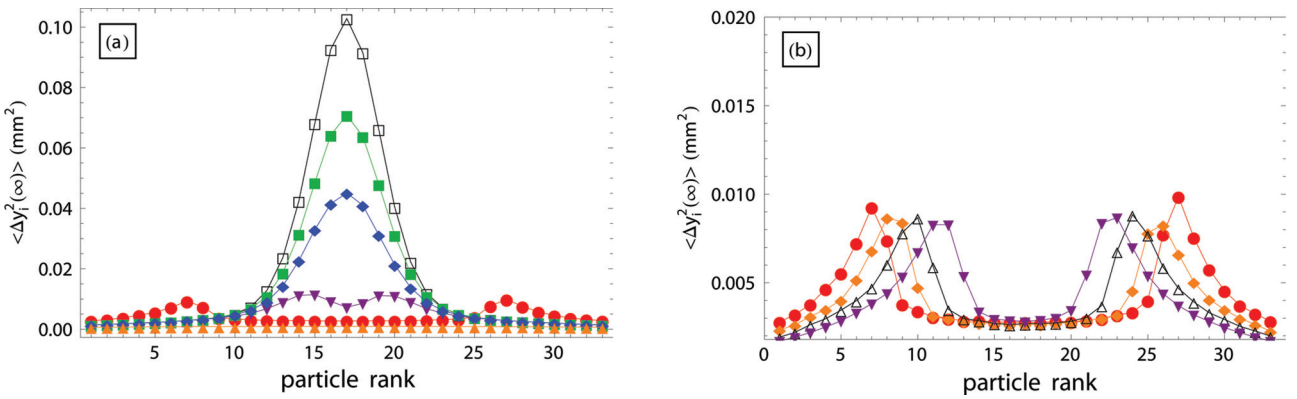

FIG. 14. (Color online) Saturation values of the transverse mean square displacement $\langle \Delta y_n^2 \rangle_{\rm sat}$ (mm^2) according to the particle index n in the RBC system at $T = 10^{11}$ K. In this configuration $\beta_{ZZ}(0) = 2.10$ N/mm; $\beta_{ZZ}(T) = 2.07$ N/mm. (a) $\beta = 1.075$ N/mm (red circles), $\beta = 2.042$ N/mm (purple triangles down), $\beta = 2.085$ N/mm (open black squares), $\beta = 2.096$ N/mm (green squares), $\beta = 2.107$ N/mm (blue diamonds), $\beta = 4.3$ N/mm (orange triangles up). (b) $\beta = 1.075$ N/mm (red circles), $\beta = 1.29$ N/mm (orange diamonds), $\beta = 1.505$ N/mm (open black triangles), $\beta = 1.72$ N/mm (purple triangles down).

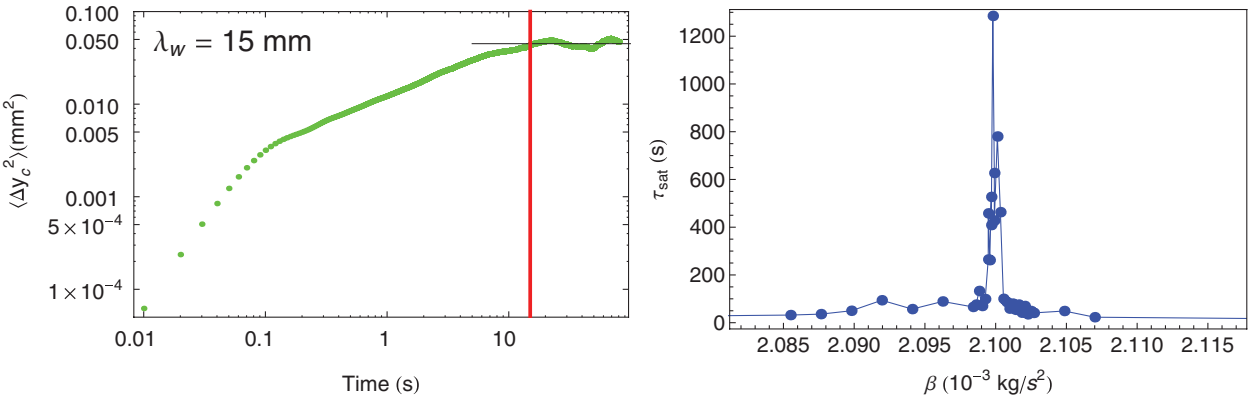

FIG. 15. (Color online) (Left) Logarithmic plot of the transverse MSD $\langle \Delta y_c(t)^2 \rangle$ for the central particle (mm^2) as a function of time in a RBC system of 33 particles at $T = 10^{11}$ K. The solid vertical red line indicates the saturation time $\tau_{\rm sat}$. (Right) Variation of the saturation time $\tau_{\rm sat}$ (s) with the transverse stiffness β (10^3 kg s^{-2}) in the same RBC system at $T = 10^2$ K. In this configuration $\beta_{ZZ}(0) = 2.10$ N/mm.

are farther apart from their neighbors than the particles outside the bubble, because in the bubble the nearest neighbor of the particle of rank n has the rank $n \pm 2$ (see Fig. 4). When β decreases, all the bubble particles roughly have the same $\langle \Delta x_n^2 \rangle_{\rm sat}$, which is smaller than at the bifurcation but still higher than for the denser particles outside the bubble. Let us also notice that whatever the value of β, the particles at the bubble edges exhibit a large $\langle \Delta x_n^2 \rangle_{\rm sat}$ since they have the farthest neighbors.

The saturation values $\langle \Delta y_n^2 \rangle_{\rm sat}$ are presented in Fig. 14. For $\beta \gg \beta_{ZZ}(0)$, they are roughly independent of the particle positions and correspond to the saturation values associated with particles confined in a quadratic potential. When β decreases, $\langle \Delta y_n^2 \rangle_{\rm sat}$ associated with the central particle strongly increases until β reaches the thermal threshold $\beta_{ZZ}(T)$. This can be observed in Fig. 14(a), for which the maximum of $\langle \Delta y_n^2 \rangle_{\rm sat}$ associated with the central particle is observed for a negative value of ϵ. The maximum value of $\langle \Delta y_n^2 \rangle_{\rm sat}$ is observed for a negative ϵ. This enhancement of $\langle \Delta y_n^2 \rangle_{\rm sat}$ for the bubble particles is due to the flips between the energetically equivalent and symmetric zigzag configurations.

For $\beta < \beta_{ZZ}(T)$, the bubble particles are trapped in one of the symmetric zigzag configurations and have smaller $\langle \Delta y_n^2 \rangle_{\rm sat}$. We can notice that the highest $\langle \Delta y_n^2 \rangle_{\rm sat}$ are associated with the particle belonging to the bubble edges [see Fig. 14(b)], as was already the case for the longitudinal fluctuations.

This result supports the fact that the bifurcation threshold can be associated with the maximum of $\langle \Delta y_n^2 \rangle_{\rm sat}$. However, the strongest effect of the bifurcation is observable on the saturation time $\tau_{\rm sat}$ of $\langle \Delta y_n^2(t) \rangle$ associated with the central particle. By definition, $\tau_{\rm sat}$ is such that

$$\left\langle \Delta y_n^2(\tau_{\rm sat}) \right\rangle \equiv \left\langle \Delta y_n^2 \right\rangle_{\rm sat}. \tag{10}$$

At low temperature, in the vicinity of $\beta_{ZZ}(0)$, the thermally activated soft mode induces very slow particle oscillations. We have previously shown that the saturation time is given by $\tau_{\rm sat} = \gamma / \Omega_{sm}^2$ [21] and diverges at the bifurcation threshold $\beta = \beta_{ZZ}(0)$.

When the temperature increases, the thermal flips become activated in the bifurcation region $\beta_{ZZ}(T) < \beta < \beta_{ZZ}(0)$. Concerning the transverse MSD behavior, these flips may be described as "oscillations" between the two symmetric equilibrium configurations with a characteristic time given by the Kramers time τ_K. This characteristic time gives the order of magnitude of $\tau_{\rm sat}$ in the bifurcation region. It becomes higher

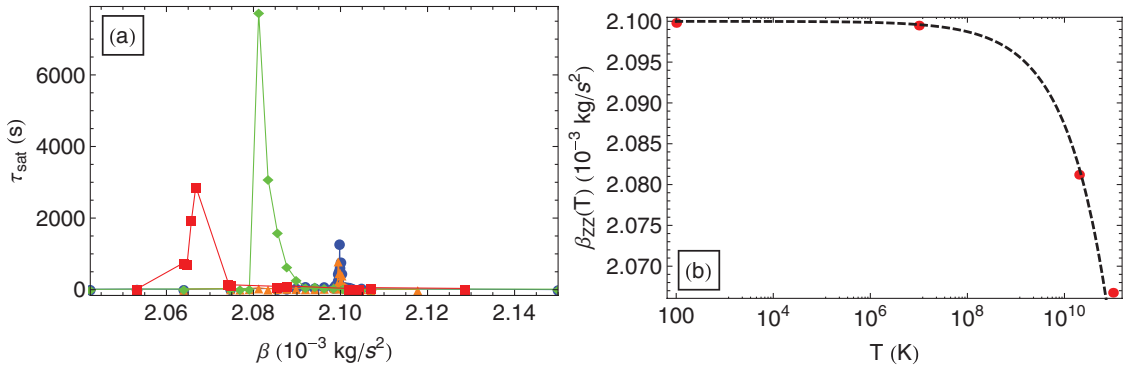

FIG. 16. (Color online) (a) Variation of the saturation time $\tau_{\rm sat}$ (s) of the transverse mean square displacement $\langle \Delta y_c(t)^2 \rangle$ for the center particle with the transverse stiffness β (10^3 kg s^{-2}), in the RBC system [$\beta_{ZZ}(0) = 2.10$ N/mm] at several temperatures: $T = 10^2$ K (blue squares; Fig. 15 is a magnification of this particular plot); $T = 10^7$ K (orange triangles up); $T = 2 \times 10^{10}$ K (green triangles down); $T = 10^{11}$ K (red disks). (b) Evolution of the thermal threshold $\beta_{ZZ}(T)$ with the temperature for this same RBC system, deduced from plot (a): $\beta_{ZZ}(10^2\ {\rm K}) = 2.0998$ N/mm; $\beta_{ZZ}(10^7\ {\rm K}) = 2.0995$ N/mm; $\beta_{ZZ}(2 \times 10^{10}\ {\rm K}) = 2.0812$ N/mm; $\beta_{ZZ}(10^{11}\ {\rm K}) = 2.06675$ N/mm. The dotted line corresponds to the scaling $\beta_{ZZ}(0) - \beta_{ZZ}(T) \propto (k_B T)^{1/2}$ proposed in Ref. [19].

and higher as β gets closer to $\beta_{ZZ}(T)$, as explained in Sec. III. Thus, at high temperature, the particle dynamics is similar to that observed at low temperature, provided the deterministic threshold is replaced with the thermal threshold.

Therefore, the thermal bifurcation threshold may be determined by following the evolution of the saturation time with the control parameter, which is the confinement parameter β in our simulations. An example is shown in the left plot of Fig. 15. After a short ballistic regime, the transverse MSD scales as $t^{1/2}$ until reaching its saturation value at a time $\tau_{\rm sat}$, which is indicated by a vertical solid red line. More details on the dynamics of the fluctuations before their saturation is provided in Ref. [21]. The plot of $\tau_{\rm sat}$ as a function of β is shown in the right plot of Fig. 15. It exhibits a very large increment of roughly three orders of magnitude when $\beta \to \beta_{ZZ}(T)$. It is also very sharp, because the large values of $\tau_{\rm sat}$ take place for a relative variation of β that is less than 0.5%. These features of the curve are consistent with an actual divergence of the saturation time. The measurement of the saturation time thus provides the most sensitive and precise measurement of $\beta_{ZZ}(T)$.

In Fig. 16(a), we plot $\tau_{\rm sat}$ as a function of β for the same system at several temperatures. The value of $\beta_{ZZ}(0)$ is thus the same in all cases, and we see that we are able to define precisely the thermal threshold $\beta_{ZZ}(T)$ on four orders of magnitude in temperature. From Fig. 16(a), we are able to measure $\beta_{ZZ}(T)$ and compare it to the predictions of noisy bifurcation theory [19]. The result is plotted in Fig. 16(b) and shows very good agreement with the theoretical predictions of Agez *et al.* [19].

VI. CONCLUSION

The studies of noisy bifurcation have shown that the fluctuations of the particle positions make the bifurcation analysis more complex. In particular, the thermal noise broadens the variations of the order parameter according to the control parameter and smooths the singularity indicating the bifurcation at $T = 0$ K. Moreover, this noise shifts the bifurcation threshold, which then depends upon the temperature. Last, the very notion of a singular bifurcation can be questioned, in favor of a blurred *bifurcation region*.

Thus, the determination of the thermal threshold is not straightforward and requires a specific procedure. In this paper we have proposed such a procedure, based on the measurement of a divergence. Due to its sharpness, it seems to offer the best opportunity to determine precisely the thermal threshold.

In order to illustrate this procedure, we have considered a system of interacting particles confined in a straight finite channel; a strong transverse parabolic confinement with a stiffness β forbids any crossing between particles. In such a system, as soon as the transverse interparticle interactions cancel the transverse confinement force, the equilibrium configuration with all particles aligned is replaced with two symmetric zigzag configurations. This configurational transition is described by the supercritical pitchfork bifurcation formalism. The study of the particle trajectories clearly shows the peculiar behaviors observed in the "bifurcation region" in which the particles can flip from one zigzag equilibrium position to its symmetric equivalent. Moreover, the analysis of the variations of the order parameter with the control parameter or that of the pair correlation function shows that the fluctuations of the particle positions near the threshold do not fulfill the ergodic assumption which is necessary to ensure the equivalence between an ensemble average and an average calculated over a finite time.

By contrast, we can take advantage of the specific behaviors of the variations with time of the MSD of the particles near the threshold, in particular the transverse MSD, to determine without any ambiguity the thermal threshold $\beta_{ZZ}(T)$. We have shown that the time required to reach the transverse MSD saturation, associated with the longest flip time in the bifurcation region, diverges when β moves towards $\beta_{ZZ}(T)$. Thus, such a divergence provides a very efficient and precise way to determine the threshold of a noisy bifurcation.

The variations of $\beta_{ZZ}(T)$ with the temperature deduced from this procedure are in very good agreement with existing theoretical predictions. This simultaneously validates both the procedure we propose and the theoretical analysis. Established here for a finite sized system, this procedure of threshold determination can be easily extended for systems with equidistant particles since, near the bifurcation, all the particles have the same behaviors.

ACKNOWLEDGMENT

We acknowledge useful discussions with Frederic van Wijland.

APPENDIX: ZIGZAG TRANSITION IN PERIODIC SYSTEMS

The normal form of the zigzag transition may be obtained explicitly for the case of a periodic system of particles [$F_c^l(x) = 0$]. In this case, all particles behave identically, and at $T = 0$ K, the equation of transverse motion of any particle is given by

$$m\langle\ddot{y}\rangle + m\gamma\langle\dot{y}\rangle = -\beta\langle y\rangle + 2\mathbf{F}_{\rm int}(\sqrt{\overline{d}^2 + 4\langle y\rangle^2})\cdot\mathbf{e}_y, \quad \text{(A1)}$$

where $F_{\rm int}$ is the force derived from the potential $V_{\rm int}$ and where $\overline{d}$ is the longitudinal interparticle distance. Since the displacement $\langle y\rangle$ is small with respect to $\overline{d}$, we may develop this equation in power law of $\langle y\rangle$. By retaining only the first nonlinear correction in $\langle y\rangle$, we obtain the normal form of the supercritical pitchfork bifurcation [45]

$$m\langle\ddot{y}\rangle + m\gamma\langle\dot{y}\rangle = a_1\langle y\rangle - a_3\langle y\rangle^3, \quad \text{(A2)}$$

where the coefficients a_1 and a_3 are given by

$$a_1 = -\beta + \frac{4F_{\rm int}(\overline{d})}{\overline{d}}, \quad a_3 = 8\left[\frac{F'_{\rm int}(\overline{d})}{\overline{d}^2} - \frac{F_{\rm int}(\overline{d})}{\overline{d}^3}\right] \leqslant 0. \quad \text{(A3)}$$

The bifurcation takes place when the confinement coefficient $\beta = \beta_{ZZ}(0) = 4F_{\rm int}(\overline{d})/\overline{d}$. Introducing $\epsilon \equiv \beta/\beta_{ZZ}(0) - 1$, the stable equilibrium configurations are given by $\langle y\rangle = 0$ for $\epsilon > 0$ and $\langle y\rangle = \pm(-a_1/a_3)^{1/2} \propto \pm(-\epsilon)^{1/2}$ otherwise. These results are consistent with previous studies which numerically [7,27] and analytically [38] show that at $T = 0$ K

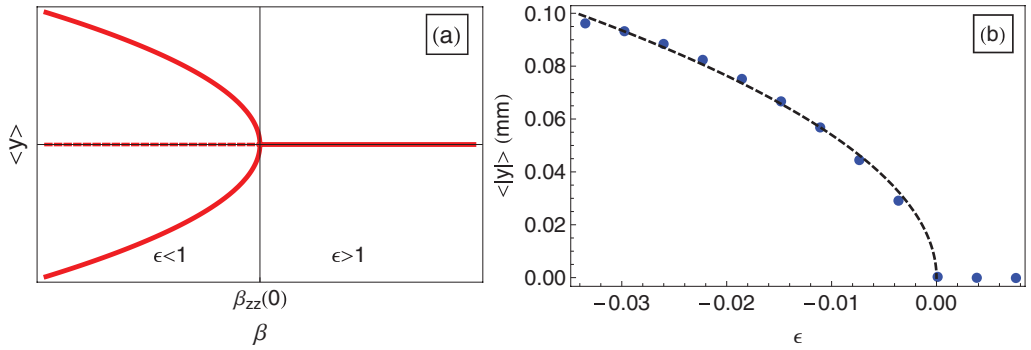

FIG. 17. (Color online) Bifurcation diagram for a periodic system. (a) Theoretical equilibrium positions $\langle y \rangle$ according the transverse confinement derived from the bifurcation equation (A2). The red solid and dotted lines correspond, respectively, to the stable and unstable positions. (b) Variations of the equilibrium position $\langle |y| \rangle$ with the dimensionless distance to the threshold, ϵ, for a periodic system of 32 particles ($L = 60$ mm). The dotted line scales as $\sqrt{-\epsilon}$.

the zigzag transition is well described in the framework of Landau second order transitions, taking, respectively, $\langle y \rangle$ and ϵ as order and control parameters [see Fig. 17(b)]. The interparticle distance may be taken as the control parameter as well. In this description the bifurcation happens when the interparticle distance is smaller than $d_{ZZ}(E_{\rm int},\beta)$ [9,28].

[1] This is not the only example of configurational phase transition that happens in such systems. Recently, Flomenbom [2] has described a clustering transition in files of non-Brownian particles.

[2] O. Flomenbom, Europhys. Lett. **94**, 58001 (2011).

[3] G. Birkl, S. Kassner, and H. Walther, Nature (London) **357**, 310 (1992).

[4] M. Mielenz, J. Brox, S. Kahra, G. Leschhorn, M. Albert, and T. Schaetz, Phys. Rev. Lett. **110**, 133004 (2013).

[5] M. G. Raizen, J. M. Gilligan, J. C. Bergquist, W. M. Itano, and D. J. Wineland, Phys. Rev. A **45**, 6493 (1992).

[6] S. L. Gilbert, J. J. Bollinger, and D. J. Wineland, Phys. Rev. Lett. **60**, 2022 (1988).

[7] G. Piacente, I. V. Schweigert, J. J. Betouras, and F. M. Peeters, Phys. Rev. B **69**, 045324 (2004).

[8] A. Melzer, Phys. Rev. E **73**, 056404 (2006).

[9] T. E. Sheridan and K. D. Wells, Phys. Rev. E **81**, 016404 (2010).

[10] B. Liu and J. Goree, Phys. Rev. E **71**, 046410 (2005).

[11] J. P. Schiffer, J. Phys. B. **36**, 511 (2003).

[12] C. Lutz, M. Kollmann, P. Leiderer, and C. Bechinger, J. Phys.: Condens. Matter **16**, S4075 (2004).

[13] Q.-H. Wei, C. Bechinger, and P. Leiderer, Science **287**, 625 (2000).

[14] B. Lin, M. Meron, B. Cui, S. A. Rice, and H. Diamant, Phys. Rev. Lett. **94**, 216001 (2005).

[15] C. Lutz, M. Kollmann, and C. Bechinger, Phys. Rev. Lett. **93**, 026001 (2004).

[16] J.-B. Delfau, C. Coste, C. Even, and M. Saint Jean, Phys. Rev. E **82**, 031201 (2010).

[17] At fixed transverse stiffness β and for a given longitudinal confinement potential (which may be equal to zero for periodic boundary conditions), the zigzag transition happens below a mean interparticle distance d_{ZZ}, that is when $N > N_{ZZ}$ at fixed system length L or when $L < L_{ZZ}$ at fixed particle number N. At fixed transverse stiffness β and fixed mean interparticle distance $\overline{d}$, the zigzag transition happens in the center of finite cells at a sufficiently large longitudinal confinement, for $\lambda_w > \lambda_w^{ZZ}$ at fixed potential amplitude E_w or for $E_w > E_w^{ZZ}$ at fixed potential characteristic length λ_w. Some examples are given in Fig. 3.

[18] C. Meunier and A. Verga, J. Stat. Phys. **50**, 345 (1988).

[19] G. Agez, M. G. Clerc, and E. Louvergneaux, Phys. Rev. E **77**, 026218 (2008).

[20] N. van Kampen, *Stochastic Processes in Physics and Chemistry* (North-Holland, Amsterdam, 1992).

[21] J.-B. Delfau, C. Coste, and M. Saint Jean, Phys. Rev. E **87**, 032163 (2013).

[22] G. Agez, C. Szwaj, E. Louvergneaux, and P. Glorieux, Phys. Rev. A **66**, 063805 (2002).

[23] G. De Chiara, A. del Campo, G. Morigi, M. Plenio, and A. Retzker, New J. Phys. **12**, 115003 (2010).

[24] D. H. E. Dubin, Phys. Rev. E **55**, 4017 (1997).

[25] T. E. Sheridan and A. Magyar, Phys. Plasmas **17**, 113703 (2010).

[26] P. Galatola, G. Coupier, M. Saint Jean, J.-B. Fournier, and C. Guthmann, Eur. Phys. J. B **50**, 549 (2006).

[27] J. P. Schiffer, Phys. Rev. Lett. **70**, 818 (1993).

[28] D. H. E. Dubin, Phys. Rev. Lett. **71**, 2753 (1993).

[29] J. E. Galvan-Moya and F. M. Peeters, Phys. Rev. B **84**, 134106 (2011).

[30] G. Piacente, G. Q. Hai, and F. M. Peeters, Phys. Rev. B **81**, 024108 (2010).

[31] J.-B. Delfau, C. Coste, and M. Saint Jean, Phys. Rev. E **85**, 041137 (2012).

[32] J.-B. Delfau, C. Coste, and M. Saint Jean, Phys. Rev. E **85**, 061111 (2012).

[33] J. Guckenheimer and P. Holmes, *Nonlinear Oscillations, Dynamical Systems, and Bifurcations of Vector Fields* (Springer-Verlag, New York, 1983).

[34] P. Manneville, *Dissipative Structure and Weak Turbulence* (Academic Press, New York, 1990).
[35] D. H. E. Dubin and J. P. Schiffer, Phys. Rev. E **53**, 5249 (1996).
[36] G. Morigi and S. Fishman, Phys. Rev. Lett. **93**, 170602 (2004).
[37] G. Morigi and S. Fishman, Phys. Rev. E **70**, 066141 (2004).
[38] S. Fishman, G. De Chiara, T. Calarco, and G. Morigi, Phys. Rev. B **77**, 064111 (2008).
[39] G. Astrakharchik, G. De Chiara, G. Morigi, and J. Boronat, J. Phys. B. **42**, 154026 (2009).
[40] J. P. Home, D. Hanneke, J. D. Jost, D. Leibfried, and D. J. Wineland, New J. Phys. **13**, 073026 (2011).
[41] J.-B. Delfau, C. Coste, and M. Saint Jean, Phys. Rev. E **84**, 011101 (2011).
[42] D. Lucena, D. V. Tkachenko, K. Nelissen, V. R. Misko, W. P. Ferreira, G. A. Farias, and F. M. Peeters, Phys. Rev. E **85**, 031147 (2012).
[43] H. Kramers, Physica **7**, 284 (1940).
[44] T. Sheridan, Phys. Scr. **80**, 065502 (2009).
[45] To be more specific, Eq. (A1) is obtained when the dynamics is reduced to the most unstable mode, which has the regular zigzag structure ($x_n = n/\rho, y_n = (-1)^n\langle y\rangle$). Then the exact normal form for the supercritical pitchfork bifurcation is obtained when the second-order differential equation Eq. (A2) is further reduced to its center manifold, dropping the slave mode which is attenuated with time constant γ^{-1}.